Electronic Supporting Information

Dual-mode sensor based on the synergy of magnetic separation and functionalized probes for the ultrasensitive detection of *Clostridium perfringens*

List of Contents:

S1. The oligonucleotides employed for this work

Table S1 The sequences for oligonucleotides employed for this work.

name	sequence (5' to 3')
DNA walker	TTTTTTTTTTTTTTTTTTTTTACAGAGCACGGGAATGTTACTGCCTGT
Aptamer	TCA ACG GCA GTA ACA TTA GC
H1	TTTTTT ACA GGC AGT AAC TAA GCC GTAGAT GTT ACT GCC ACG TGC GGA
H2	TTTTTTCCG TCA TTGATT CGG CAT CTA CAA TGA CGG
Trigger DNA	TACTTTGCCTATCC GCA CGT
H3	AA-GGTTGTATAGTAGGCAAAGTAACTATACAACCTACTACCTCA
H4	ACTTTGCCTACTATACAATGAGGTAGTAGGTTGTATAGTAGG-AA
CPAF1	GCT AAT ACT GCC GTT GA
CPAR1	CCT CTG ATA CAT GTA AG
CPAF2	GCT TAT TTG TGC CGC GCT A
CPAR2	CAT AGC ATC AGT TCC TGT TCC A
AlphaF	GAT TGA TGG AAC AGG AAC TC
AlphaR	ACG GCA GTA ACA TTA GCA
PlcF	TTG GAG AGG CTA TGC ACT ATT TT
plc	CTT AAC ATG TCC TGC GCT ATC A

S2. The comparison between different detection methods for sensing C. perfringens

Table S2 The comparison between different methods for detecting *C. perfringens.*

Method	System	Detection range	LOD	Assay time	reference
LAMP	-	0 ~ 1.2 × 10^8 CFU mL^{-1}	12 CFU/mL	12 h	[1]
Electrochemiluminescence	gold electrode (rolling circle amplification)	10^{-15} ~ 10^{-9} M	10^{-15} M	Approximately 1 h	[2]
DPV	SA/ADH/Fe_3O_4 nanocomposites	10^{-12} ~ 10^{-6} M	10^{-12} M	Same as PCR	[3]
EIS	CeO_2/chitosan/GCE	10^{-14} ~ 10^{-7} M	7.06 × 10^{-15} M	-	[4]
PCR and RPA	Real-time PCR and real-time RPA	2 ~ 1.0 ×10^{10} CFU mL^{-1}	2 CFU mL^{-1}	14 ~ 46 min	[5]
LAMP-LFB	-	0.01 ~ 10^6 CFU mL^{-1}	10 CFU g^{-1}	24 h	[6]
PSR	-	80 ng μl^{-1} ~ 0.8 fg μl^{-1}	80 fg μl^{-1}	Same as PCR	[7]
DPV	DNA walker/HCR/MGCE	1 ~ 10^8 CFU mL^{-1}	1 CFU mL^{-1}	8 h	This work

*RPA: Polymerase Amplification Assays; LAMP-LFB: loop-mediated isothermal amplification in combination with a lateral-flow biosensor; PSR: polymerase spiral reaction.

S3. Diffusion of the biosensor

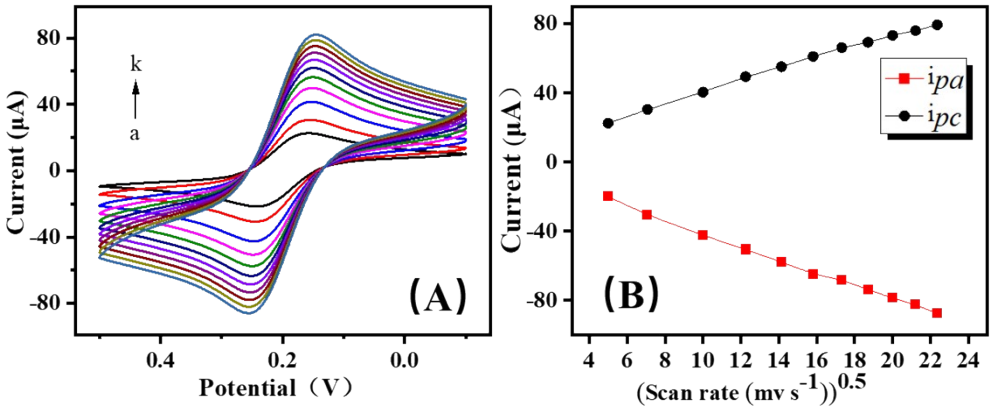

Fig. S1. (A) CVs of the DNA biosensor in electrolyte solution at different scan rates of (a) 25, (b) 50, (c) 100, (d) 150, (e) 200, (f) 250, (g) 300, (h) 350, (i) 400, (j) 450, and (k) 500 mV/s. (B) The linear relationship between the peak value and the square root of different scanning rates. 4lg CFU/mL of *C. perfringens* was used.

S4. Optimization of the electrochemical sensor

There is no doubt that the sensitivity of the sensor depends not only on the synergistic strategy but also on the embed of MB. On the other hand, aptamer are the bridges for communication between dual-mode sensors. What's more important, time is particularly important for biosensor, as well. In recent years, in the research of DNA sensors, the construction process of sensors is mostly carried out at conventional room temperature; and the pH is around 7.0. This is because the acidic or alkaline buffer may damage the structure of the DNA strand. Therefore, in order to carry out the experiment smoothly, the sensor construction temperature of this experiment is 25 ℃, and the buffer pH is adjusted to 7.0 [8-12]. Therefore, the concentration of aptamer; The concentration of MB; The time of MB participating in the reaction, and the dosage of CMBS were optimized.

As shown in Fig. S2A, the molarity Aptamer was investigated. the concentration of Aptamer gradually decreased, and the DPV signal decreases accordingly, the attenuation is attributed to that insufficient amount of Aptamer added to modify the binding site exposed by DNA walker on the CMB surface, which is then bound by

bovine serum protein in the subsequent blocking reaction, resulting in reduced DPV signal. Thus, 1 μM is selected as the Aptamer dosage.

As one of the signal enlargement strategies of this sensor, the application of MB optimizes the reaction concentration and reaction time of MB. As shown in Figures S2B and C, with the increase of MB concentration and reaction time, the electrical signal increases gradually. When MB concentration reaches 10 μM and reaction time reaches 60 min, the electrical signal does not increase but becomes stable. This trend is due to the full incorporation of MB into the DNA chain structure. Thus, a concentration of 10 μM MB and a reaction time of 60 min were selected as the optimal conditions.

As the basis of this dual-mode sensor, the amount of CMBs is also worth considering. As shown in Fig. S2D, with the continuous increase of the amount of CMBs, the peak value of the electrical signal increases. When the amount of CMBs increases to 10 μL. This trend is gradually gentle, and the increase of the peak value of the electric signal is decreasing. Therefore, 10 μL as the optimum condition.

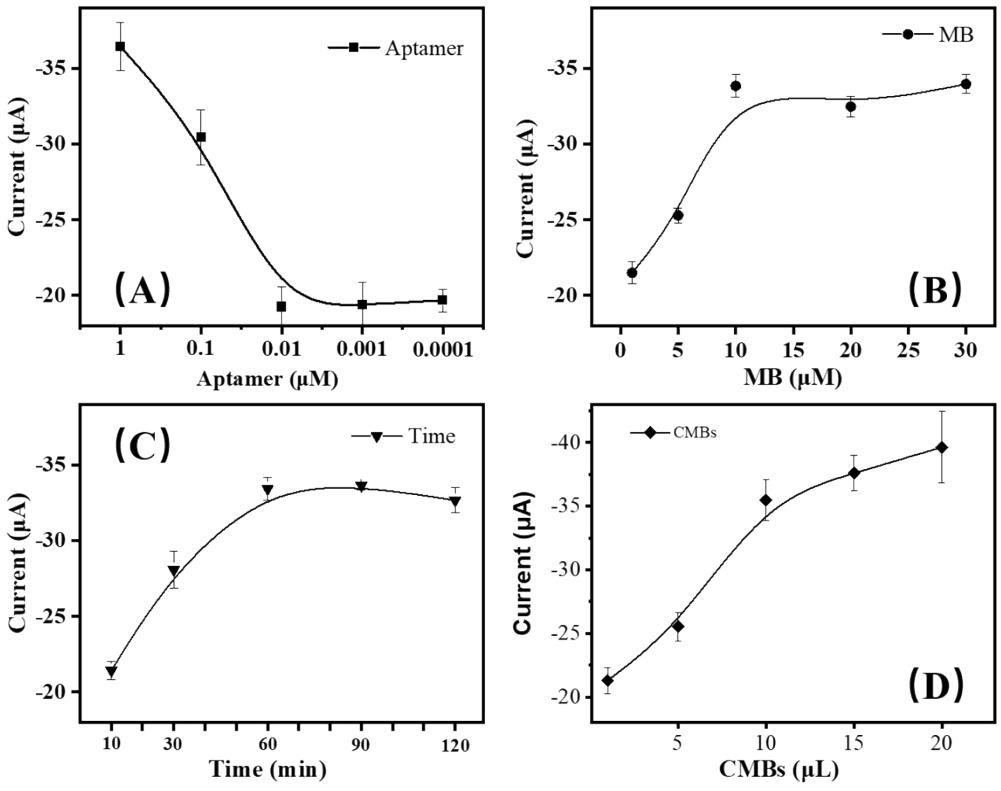

Fig S2. Optimization of experimental conditions (A) Concentration of aptamer: 1,

0.1, 0.001, 0.0001 μM; (B) Concentration of MB: 0, 5, 10, 20, 30 μM; (C) Reaction time of MB: 10, 30, 60, 90, 120 min; (D) Addition amount of CMBs: 1, 5, 10, 15, 20 μL. 4lg CFU/mL *C. perfringens* was used. Error bars showed the standard deviation of three experiments.

reference

1. G. B. Priya, R. K. Agrawal, A. A. P. Milton, M. Mishra, S. K. Mendiratta, R. K. Agarwal, A. Luke, B. R. Singh, and D. Kumar, *Anaerobe*, 2018, **54**, 178-187, DOI: 10.1016/j.anaerobe.2018.09.005.
2. D. N. Jiang, F. Liu, C. Liu, L. L. Liu, Y. Li and X. Y. Pu, *Analytical Methods*, 2014, **6**, 1558-1562, DOI: 10.1039/C3AY41961D.
3. D. N. Jiang, F. Liu, L. Q. Zhang, L. L. Liu, C. Liu, and X. Y. Pu, *Rsc Advances*, 2014, **4**, 57064-57070, DOI: 10.1039/C4RA09834J.
4. X. Qian, Q. Qu, L. Li, X. Ran, L. Zuo, R. Huang, and Q. Wang, *Sensors*, 2018, **18**, 1878, DOI: 10.3390/s18061878.
5. L. Liu, R. Li, Z. Chen, J. Wang, X. Sun, W. Yuan and J. Wang, *Food Science*, 2020, **41**, 268-272, DOI: 10.7506/spkx1002-6630-20181026-307.
6. T. Sridapan, W. Tangkawsakul, T. Janvilisri, W. Kiatpathomchai, S. Dangtip, N. Ngamwongsatit, D. Nacapricha, P. Ounjai and S. Chankhamhaengdecha, *Plos One*, 2021, **16**, e0245144, DOI: 10.1371/journal.pone.0245144.
7. A. A. P. Milton, K. M. Momin, S. Ghatak, G. B. Priya, M. Angappan, S. Das, K. Puro, R. K. Sanjukta, I. Shakuntala, A. Sen and B. K. Kandpal, *Heliyon*, 2021, **7**, e05941, DOI: 10.1016/j.heliyon.2021.e05941
8. W. Zhang, P. Zhang, Y. Liang, W. Cheng, L. Li, H. Wang, Z. Yu, Y. Liu, and X. Zhang, RSC Advances, 2022, **12**, 13448-13455, DOI: 10.1039/D2RA01817A.
9. N. D. Md. Sani, E. Y. Ariffin, W. Sheryn, M. A. Shamsuddin, L. Y. Heng, J. Latip, S. A. Hasbullah and N. I. Hassan, Sensors, 2019, **19**, 5111, DOI: 10.3390/s19235111.
10. J. Jeong, H. Kim, D. J. Lee, B. J. Jung, and J. B. Lee, Nanoscale Research Letters, 2016, **11**, 242, DOI: 10.1186/s11671-016-1440-7.
11. Y. Mao, Y. Chen, S. Li, S. Lin, and Y. Jiang, Sensors, 2015, **15**, 28244-28256, DOI: 10.3390/s151128244
12. E. Yuhana Ariffin, L. Y. Heng, L. L. Tan, N. H. Abd Karim and S. A. Hasbullah, Sensors, 2020, **20**, 1279, DOI: 10.3390/s20051279.